


RESEARCH ARTICLE

Respiratory magnetic resonance imaging biomarkers in Duchenne muscular dystrophy

Ami Mankodi¹ , William Kovacs², Gina Norato³, Nathan Hsieh², W. Patricia Bandettini⁴, Courtney A. Bishop⁵, Hირy Shimellis¹, Rexford D. Newbould⁵, Eunhee Kim³, Kenneth H. Fischbeck¹, Andrew E. Arai⁴ & Jianhua Yao²

¹Neurogenetics Branch, National Institute of Neurological Disorders and Stroke, National Institutes of Health, Bethesda, Maryland

²Radiology and Imaging Sciences, The National Institutes of Health Clinical Center, Bethesda, Maryland

³Office of Biostatistics, National Institute of Neurological Disorders and Stroke, National Institutes of Health, Bethesda, Maryland

⁴Advanced Cardiovascular Imaging, National Heart Lung and Blood Institute, National Institutes of Health, Bethesda, Maryland

⁵Imanova Center for Imaging Sciences, Imperial College London, Hammersmith Hospital, London, United Kingdom

Correspondence

Ami Mankodi, Hereditary Muscle Disease Unit, Neurogenetics Branch, NINDS, NIH, 35 Convent Drive, Building 35, Room 2A-1002, Bethesda, MD 20892-3075. Tel: 301 827 6690; Fax: 301 480 3365; E-mail: Ami.Mankodi@nih.gov

Funding Information

The study was supported by the Intramural Research Program of the National Institute of Neurological Disorders and Stroke, the National Institutes of Health Clinical Center, and the National Heart, Lung, and Blood Institute, National Institutes of Health, Bethesda, Maryland

Received: 28 May 2017; Accepted: 28 June 2017

Annals of Clinical and Translational Neurology 2017; 4(9): 655–662

doi: 10.1002/acn3.440

Introduction

Duchenne muscular dystrophy (DMD) is the most common inherited myopathy and characterized by progressive weakness of skeletal, cardiac, and respiratory muscles. Respiratory failure is inevitable in DMD.¹ Multidisciplinary care and ventilatory support have increased longevity,^{2,3} and corticosteroids and idebenone may stabilize the respiratory function in nonambulatory patients.^{4,5} Restoration of the diaphragm function alone prevented cardiomyopathy in mice.⁶ Thus, the diaphragm and other respiratory muscles remain the important therapeutic targets in DMD.

Abstract

Objective: To examine the diaphragm and chest wall dynamics with cine breathing magnetic resonance imaging (MRI) in ambulatory boys with Duchenne muscular dystrophy (DMD) without respiratory symptoms and controls. **Methods:** In 11 DMD boys and 15 controls, cine MRI of maximal breathing was recorded for 10 sec. The lung segmentations were done by an automated pipeline based on a Holistically-Nested Network model (HNN method). Lung areas, diaphragm, and chest wall motion were measured throughout the breathing cycle. **Results:** The HNN method reliably identified the contours of the lung and the diaphragm in every frame of each dataset (~180 frames) within seconds. The lung areas at maximal inspiration and expiration were reduced in DMD patients relative to controls ($P = 0.02$ and <0.01 , respectively). The change in the lung area between inspiration and expiration correlated with percent predicted forced vital capacity (FVC) in patients ($r_s = 0.75$, $P = 0.03$) and was not significantly different between groups. The diaphragm position, length, contractility, and motion were not significantly different between groups. Chest wall motion was reduced in patients compared to controls ($P < 0.01$). **Interpretation:** Cine breathing MRI allows independent and reliable assessment of the diaphragm and chest wall dynamics during the breathing cycle in DMD patients and controls. The MRI data indicate that ambulatory DMD patients breathe at lower lung volumes than controls when their FVC is in the normal range. The diaphragm moves normally, whereas chest wall motion is reduced in these boys with DMD.

Current guidelines emphasize the need for timely diagnosis of respiratory complications in DMD.^{3,7} Most patients are not aware of their loss of respiratory muscle strength until a respiratory infection leads to pneumonia. Annual forced vital capacity (FVC) assessments are recommended. The FVC usually increases with age through 10 years and plateaus before declining after age 18 years in DMD patients.⁸ It has a poor specificity for the respiratory muscle weakness.^{8,9} A $>25\%$ postural FVC drop may indicate diaphragm weakness.¹⁰ However, postural FVC drop is not seen in DMD patients because they have more generalized weakness affecting other inspiratory muscles than the diaphragm.¹¹

Pulmonary function tests do not distinguish the specific involvement of different respiratory muscles. Magnetic resonance imaging (MRI) has been used for detection of the diaphragm weakness in Pompe disease.^{12,13} However, the temporal resolution required for the dynamic assessment often leads to poor spatial resolution and makes the image analysis challenging. We developed a novel automated analysis pipeline and examined respiratory muscle dynamics with cine breathing MRI in ambulatory DMD boys and controls.

Subjects and Methods

Participants and study design

In this cross-sectional study, the cine breathing MRI was obtained in ambulatory subjects with DMD and healthy volunteer boys. All patients were on oral corticosteroids with a dose equivalent to prednisone 0.75 mg/kg per day. The patients travelled to the NIH Clinical Center during the screening phase of a clinical trial evaluating an oligonucleotide therapy (NCT01462292). A sitting FVC was measured before randomization into the clinical trial, which was within 3 weeks of the imaging. The controls were recruited from the NIH Clinical Research Volunteer Program registry. Subject eligibility and inclusion and exclusion criteria have been described elsewhere.¹⁴ The subjects did not have dyspnea at rest or on exertion, chest pain, need for ventilator assistance, sleep disturbances, pneumonia, swallowing difficulty, or scoliosis. None had acute illness during a month before their visit. All subjects had normal left ventricular function.¹⁵

Standard protocol approvals, registrations, and consents

The study was registered on clinicaltrials.gov (NCT01451281) and was in compliance with the NIH Privacy Act and approved by an NIH Institutional Review Board. Informed written assent and consent were obtained from each subject and parent or guardian before participation in the study.

MRI acquisition

MR images of the respiratory muscles were acquired on 1.5T scanners (Siemens Avanto or Espree, Erlangen, Germany). An 18-element torso phased array coil was used. Before the MRI scan, the participants were encouraged to practice the vital capacity maneuver in the supine position. Dynamic motion of the chest wall and diaphragm was imaged in a sagittal plane passing through the right midclavicular line, a coronal plane, and axial planes at the

tracheal bifurcation and the diaphragm levels. Cine MRI was recorded for 10 sec with the average time difference of 0.065 sec between frames for each plane. Real-time cine imaging was acquired using a balanced steady-state free precession sequence with parallel imaging acceleration as previously reported.¹⁶ The sequence parameters were repetition time 3.1 msec, echo time 1.4 msec, gradient echo train length 23, excitation flip angle 50°, slice thickness 6 mm, and a field of view 360 × 270 mm².

MRI analysis

Lung segmentation using deep learning-based approach

Deep learning is a representation learning method that allows a machine to be fed raw data and to automatically discover the representation needed for an object detection.¹⁷ We used Holistically-Nested Network (HNN),¹⁸ a deep learning model for the lung segmentation. Details of our lung segmentation method have been described elsewhere (W. Kovacs et al., unpubl. ms.). In brief, the model was constructed by training on a randomly selected frame from each MRI dataset. The initial network structure was based on a VGGNet model,¹⁹ pretrained on ImageNet,²⁰ and then fine-tuned (as in ref. 21) on a randomly selected frame of each cine breathing MRI dataset with a learning rate of 10⁻⁶. The trained model was subsequently applied to the entire set of frame sequences (typically 180 frames) in each dataset to define the contours of the lung and the diaphragm. The investigators were blinded to other clinical information.

Measurements of the lung area and the diaphragm and chest wall motion

The coronal plane provided a demonstration of symmetry of the diaphragm dome motion during the breathing cycle (Video S1). It was difficult to identify the appropriate axial plane in young children and axial images sometimes included the heart and major blood vessels. Subsequently, the sagittal plane in the right lung was chosen for further evaluation to avoid the interference of the heart with the segmentations (Video S2).

The area within the lung contour was automatically measured (Fig. 1A and B). The distances from the apex of the lung to the diaphragm at the anterior (ANT) and posterior (POST) costophrenic angles and the distance of a vertical line dropped from the apex of the lung to the diaphragm (central; CNT) were measured as described previously.²² The diaphragm length was measured along the dome of the diaphragm during inspiration. The diaphragm length was calculated as the sum of the lengths of

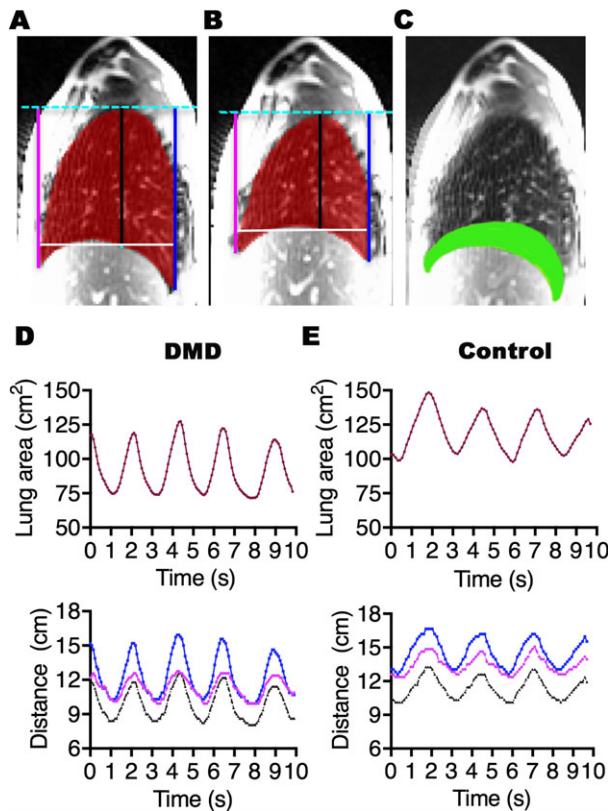


Figure 1. Representative lung segmentations and changes in the lung area and the diaphragm position relative to the thoracic apex over time. Right sagittal images show the lung segmentations (red) and the anterior (magenta), central (black), and posterior (blue) distances between the thoracic apex and the diaphragm at maximal inspiration or total lung capacity (A) and maximal expiration or residual volume (B) of the same subject. The superimposed image (C) of A and B shows the area displaced by the diaphragm motion (green). Note that the HNN method detects the entire length of the diaphragm including the dome and zones of opposition. Graphs show changes in the lung area (red; top panel) and the anterior (magenta), central (black), and posterior (blue) distances (bottom panel) in a 9-year old individual with DMD (D) and an age-matched healthy volunteer boy (E) during 10 sec (s) of dynamic MRI recording of maximal breathing. Three complete breathing cycles of maximal inspiration to maximal expiration are shown for each subject. The changes in the lung area follow the same direction as the changes in the distances during a breathing cycle in the patient and the control. All parameters are reduced in the patient compared to the control.

the diaphragm dome and the zones of apposition during expiration. The lung area, the diaphragm length, and all distances were computed in every frame of each cine MRI dataset. The frames with the maximum and minimum lung area from a breathing cycle were identified as representing maximal inspiration (Fig. 1A) and expiration (Fig. 1B), respectively. The difference between the two largest values of the lung area delta (the lung area at

maximal inspiration minus lung area at maximal expiration) was used to investigate breathing cycle effort consistency within a subject. The diaphragm motion (DM) and the chest wall motion (CWM) were calculated on the superimposed frames of the maximal inspiration and expiration from each breathing cycle as described previously.¹³ The DM was measured as the area displaced by the diaphragm, defined as the area bordered by the contours of the diaphragm in maximal expiration and maximal inspiration frames on superimposed images (Fig. 1C). The CWM was calculated by subtraction of the area displaced by the diaphragm from the lung area in maximal inspiration frame. The investigators were blinded to other clinical information.

Manual segmentation

Manual tracing of the diaphragm was done with the help of the software Analyze 11.0 on every single frame of each cine MRI dataset by an investigator (C.A.B.), who was blinded to other clinical information. The averages of closest distances between the traced diaphragm by HNN method and the manual drawing for every pixel in every frame were measured for comparison.

Statistical analysis

Wilcoxon rank sum tests were used to summarize the subject characteristics and compare the MRI measures between groups. Wilcoxon signed-rank tests were used to evaluate the difference between the two largest lung area delta values in each subject. The degree of agreement for tracing of the diaphragm between manual and HNN methods was measured by the Bland–Altman method.²³ The consistency for breath effort between breathing cycles was measured by using the intraclass correlation coefficient. Spearman's correlation coefficient (r_s) was used to assess the association between the respiratory MRI measures and subject age, height, and weight within each group. Two-sided tests were performed for all statistical analyses and the level of significance was set at $P < 0.05$. Data analyses were carried out using R version 3.3.1 (R Foundation for Statistical Computing, Vienna, Austria).

Results

Subject demographics

The dynamic respiratory muscle cine MRI was analyzed in 11 ambulatory boys with DMD (age range: 6–14 years) and 15 healthy volunteer boys (age range: 7–12 years). The patient and control groups were not significantly different in age ($P = 0.06$) or weight ($P = 0.10$) (Table 1).

Table 1. Demographics of individuals with Duchenne muscular dystrophy (DMD) and healthy volunteer boys (controls).

	DMD (<i>n</i> = 11), median (IQR)	Controls (<i>n</i> = 15), median (IQR)	<i>P</i> -value (Wilcoxon rank sum)
Age (years)	8.0 (7.0–9.5)	10.0 (9.0–11)	0.06
Height (cm)	123.8 (121.2–130.2)	143.5 (141.3–149.5)	<0.01
Weight (kg)	31.1 (27.7–38.2)	37.8 (32.4–43.9)	0.10

The DMD participants were shorter than the healthy volunteers ($P < 0.01$).

Real-time respiratory MRI measures during the vital capacity maneuver in DMD patients and controls

In 10 sec, images for 1–3 breaths were recorded in DMD boys and controls. Representative changes in the lung area and the diaphragm movement during recorded breathing cycles are shown in a 9-year-old patient and an age-matched control (Fig. 1D and E). As shown, the diaphragm moved in parallel with the changes in the lung area during a breathing cycle in each subject. The domes of the diaphragm moved symmetrically and we did not observe any paradoxical motion of the diaphragm in patients and controls (Video S1 and Video S2).

Among 9 patients and 12 controls who recorded more than a single breath, the median difference between the two largest lung area delta values was 2.1 cm² and 3.2 cm² (IQR = 1.8–4.8 cm² and 1.5–8.3 cm²), respectively. There was a significant difference between the two largest lung area delta values in the controls ($P = 0.03$), but not in the patients ($P = 0.43$). Additionally, the intra-class correlation coefficients for the lung area delta were 0.97 for the DMD group and 0.62 for the control group. Due to this difference in breath consistency between the groups, we used the MRI measures obtained during the breathing cycle with the largest lung area delta representing their best breath effort cycle in further analysis.

We found a significant difference in the lung area between the groups (Table 2). In all but one patient, the lung area at maximum inspiration and expiration was smaller than the median value of the control group (Fig. 2A and B). The lung area delta was not significantly different between the groups ($P = 0.68$; Table 2). The lung area delta correlated positively with the percent predicted FVC of patients ($r_s = 0.75$, $P = 0.03$, $n = 8$). The median percent predicted sitting FVC was 95% (range: 80–123%) in eight patients. Other three patients were not

randomized to the clinical trial and did not have FVC measured.

The CWM was reduced in all but one patient compared to the median value of the control group (Fig. 2C). The DM was greater than the median control value in all but four patients (Fig. 2D).

The mean difference in the distance between the tracing of the diaphragm by manual and the HNN segmentation methods in the same frame ($n = 3280$ frames) was 2 mm within the 95% limits of agreement (1.5, 2.6). The diaphragm length was similar between the groups during maximal inspiration and expiration. The diaphragm contractility, measured as the diaphragm length during maximal inspiration normalized to that during maximal expiration, was not significantly different between patients and controls (Table 2). The diaphragm movement, measured as the changes in the ANT, CNT, and POST distances between maximal expiration and maximal inspiration, was not significantly different between the groups.

We observed a negative correlation between age and the MRI measures of the expiration lung area and ANT, CNT, and POST distances during expiration, the diaphragm contractility, and CWM in patients but not in controls; however, these correlations were not statistically significant (Table 3). There was also a trend for a positive correlation between the lung area and the height and weight of subjects. The lung area during maximal inspiration and maximal expiration correlated positively with the corresponding ANT, CNT, and POST distances (as in ref 22) and with CWM (Table 3). The lung area during maximal inspiration but not expiration significantly positively correlated with the DM. The CWM did not significantly correlate with DM ($r_s = 0.29$, $P = 0.39$).

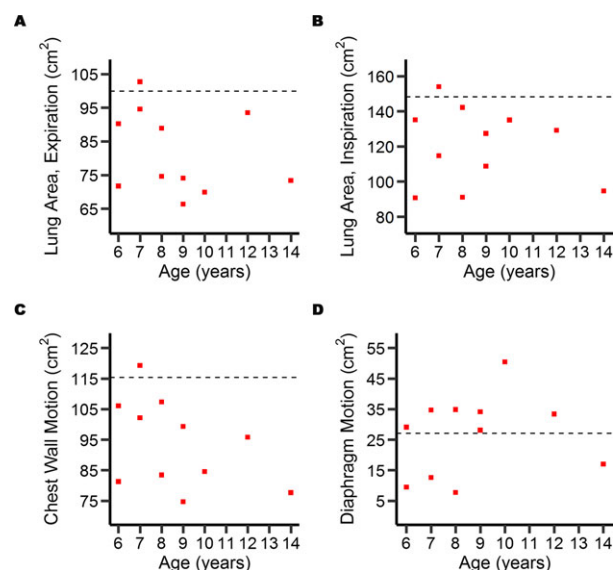
Discussion

Promising new therapies are being developed for DMD. In order for therapies to show efficacy at an early stage in the disease process, the clinical trials need to involve younger patients. The trial endpoints should be sensitive enough to demonstrate the changes in the time frame of the study. In this area, respiratory muscle function has seen little attention in clinical trials with ambulatory DMD boys. We show here that cine breathing MRI is an efficient noninvasive method for a direct assessment of the respiratory muscles in DMD patients.

We have developed a time-saving HNN method for the lung segmentation required for geometric measures and respiratory motion analysis. Although the manual segmentation method was tedious and time-consuming, the HNN method reliably identified the diaphragm and lung contours in hundreds of MR images in each dataset in

Table 2. MRI measures of the lung area, and the diaphragm and chest wall motion in individuals with Duchenne muscular dystrophy (DMD) and healthy volunteer boys (controls).

	DMD (<i>n</i> = 11), median (IQR)	Controls (<i>n</i> = 15), median (IQR)	<i>P</i> -value (Wilcoxon rank sum)
Lung area Insp ¹ (cm ²)	127.3 (101.7–135.1)	148.2 (130.4–156.2)	0.02
Lung area Exp ² (cm ²)	74.6 (72.5–91.9)	99.9 (90.0–107.3)	<0.01
Lung area delta ³ (cm ²)	42.4 (20.7–52.3)	42.3 (35.7–48.0)	0.68
ANT distance Insp (cm)	12.6 (11.8–13.8)	15.3 (14.5–16.2)	<0.01
ANT distance Exp (cm)	10.7 (9.7–12.0)	13.2 (11.9–14.5)	<0.01
ANT distance delta (cm)	2.1 (1.2–2.4)	2.3 (2.1–2.6)	0.18
POST distance Insp (cm)	15.8 (12.5–16.2)	17.4 (16.7–18.5)	<0.01
POST distance Exp (cm)	11.3 (10.3–12.0)	13.7 (12.7–14.3)	<0.01
POST distance delta (cm)	3.9 (1.7–4.7)	3.8 (3.3–4.5)	0.88
CNT distance Insp (cm)	12.6 (10.6–13.5)	14.4 (13.1–15.1)	0.02
CNT distance Exp (cm)	8.8 (8.5–10.3)	11.3 (10.3–11.9)	<0.01
CNT distance delta (cm)	3.5 (1.9–3.7)	2.9 (2.6–3.2)	0.55
Diaphragm length ⁴ Insp (cm)	14.2 (13.7–14.9)	14.0 (13.1–15.0)	0.65
Diaphragm length ⁴ Exp (cm)	21.6 (20.1–24.7)	21.8 (19.9–22.8)	0.75
Diaphragm length ⁴ Insp/Exp (%)	68.3 (62.7–69.9)	65.3 (63.2–70.7)	0.92
Diaphragm motion (cm ²)	29.1 (14.8–34.4)	27.1 (20.1–30.5)	0.84
Chest wall motion (cm ²)	95.8 (82.3–104.1)	115.4 (101.6–125.0)	<0.01

¹Insp = Inspiration.²Exp = Expiration.³Delta = change in the measure between maximum inspiration frame and maximum expiration frame in each breath cycle.⁴DMD participants *n* = 9, controls = 12.**Figure 2.** MRI quantification of the lung area, the diaphragm and chest wall motion in individuals with DMD and healthy volunteer boys. Scatter plots show that the lung area at maximal expiration (A) and at inspiration (B) are reduced in all but one of the patients (red squares) compared to the respective median value in controls (dashed line). The chest wall motion is reduced in all but one patient (C), whereas the diaphragm motion is increased in all but four patients (D) compared to the respective median control value.

average time of 45 sec using a high-performing computer clusters with 16 CPUs and 2 GPUs. The learning-based approach can be readily adapted to images acquired at different centers or using different scanning parameters. All that is needed is a new training set that can be used to train a model suitable for the new study. An advantage of using the HNN method is that as more MRI data are processed, it will become more robust through further training. Our methods show promise as useful tools for the assessment of the diaphragm and chest wall motion and identification of the causes underlying respiratory dysfunction. These tools are important to better understand the disease severity, the natural history of the disease, selection of the clinical endpoints in trials, time to initiate the treatment, and the nature of specific therapies in other neuromuscular disorders where respiratory dysfunction is a common feature.

The relatively younger DMD patients (80% of patients ≤ 10 years of age) did not have signs or symptoms of respiratory disease and had %FVC within the normal range. Previously, the lung area measured by MRI was shown to be linearly related to the spirometry lung volumes in healthy individuals and in patients with neuromuscular weakness.^{13,22} In agreement with these studies, we found that the lung area delta representing the lung area change between maximal inspiration (total lung capacity) and the

Table 3. Spearman's correlations between age, height, weight, and MRI measures of the lung area (cm²), the distances of the diaphragm from the thoracic apex (ANT, POST, and CNT; cm), diaphragm contractility (diaphragm length Insp/Exp; %), chest wall motion (CWM; cm²), and diaphragm motion (DM; cm²) in individuals with Duchenne muscular dystrophy and healthy volunteers.

	Age	Weight	Height	Lung area Insp ¹	Lung area Exp ²
Individuals with Duchenne muscular dystrophy (n = 11)					
Lung area Insp	-0.08	0.47	0.11	-	0.52
Lung area Exp	-0.34	0.48	0.56	0.52	-
ANT Insp	-0.23	0.06	-0.06	0.67 ³	0.57
ANT Exp	-0.52	0.05	0.20	0.34	0.79 ⁴
POST Insp	0.05	0.35	-0.09	0.87 ⁴	0.37
POST Exp	-0.35	0.35	0.22	0.59	0.83 ⁴
CNT Insp	-0.23	0.17	-0.04	0.85 ⁴	0.57
CNT Exp	-0.56	0.25	0.31	0.41	0.94 ⁴
Diaphragm contractility ⁵	-0.61	-0.28	0.27	-0.17	0.43
CWM	-0.44	0.49	0.15	0.83 ⁴	0.80 ⁴
DM	0.27	0.35	-0.06	0.79 ⁴	-0.03
Healthy volunteers (n = 15)					
Lung area Insp	0.16	0.41	0.47	-	0.77 ⁴
Lung area Exp	0.11	0.22	0.31	0.77 ⁴	-
ANT Insp	0.37	0.31	0.58 ³	0.81 ⁴	0.80 ⁴
ANT Exp	0.28	0.22	0.47	0.74 ⁴	0.91 ⁴
POST Insp	0.32	0.36	0.49	0.72 ⁴	0.72 ⁴
POST Exp	0.14	0.08	0.19	0.65 ⁴	0.81 ⁴
CNT Insp	0.34	0.18	0.48	0.68 ⁴	0.70 ⁴
CNT Exp	0.22	0.13	0.34	0.70 ⁴	0.82 ⁴
Diaphragm contractility ⁵	0.14	0.15	-0.05	-0.03	0.33
CWM	0.00	0.26	0.29	0.91 ⁴	0.75 ⁴
DM	0.02	0.24	0.24	0.33	0.07

¹Inspiration.

²Expiration.

³*P* < 0.05.

⁴*P* < 0.01.

⁵DMD participants *n* = 9, controls *n* = 12.

end of maximal expiration (residual volume) linearly correlated with percent predicted FVC in the DMD patients. The lung area delta was not significantly different between the patients and controls. At this early stage the MRI studies indicate that the patients had low-volume breathing compared to the controls. It has been proposed that expiratory muscles are affected early in DMD, which would lead to larger residual volumes.^{24,25} However, we observed that the lung area at residual volume was reduced indicating a change in the chest wall compliance in the patients.²⁶ Reduced lung area in patients may be at least in part related to their shorter height compared to controls.²⁷ A formal investigation into the degree of height confounding the lung area measurements is best reserved for a larger dataset.

The MRI measures of the diaphragm and chest wall motion correlated with the lung area during inspiration, indicating that both the intercostal muscles and the diaphragm are important contributors to the lung expansion in patients and controls. Previous studies showed that measurements of the FVC and inspiratory pressures may not be sufficient to detect diaphragm weakness in DMD patients due to generalized respiratory muscle weakness, and invasive tests for example, transdiaphragmatic pressure during sniff may be required.¹¹ Ultrasonography has been used to detect diaphragm weakness in patients and in animal models of DMD.^{28,29} However, MRI offers distinct advantages as it allows analysis of the diaphragm motion at defined locations in a reproducible manner and provides assessments of the diaphragm and thoracic muscles simultaneously and independently, which is necessary in order to understand the kinetics of the respiratory pump.³⁰ Previous studies have shown that the diaphragm is affected early in patients with Pompe disease.^{13,31} We found that the diaphragm function was preserved in younger DMD patients, whereas the chest wall movement (mainly intercostal muscles) was reduced during maximal inspiration. The reduction in the chest wall motion may also be related to alterations in the elasticity of the lungs associated with diminished lung volumes.³² Note that our patients did not have parenchymal lung disease, thoracic spine kyphoscoliosis, or congestive heart failure,¹⁵ which are known to cause reduction in residual volume.

The MRI methods were dependent on the ability of the participants to perform the vital capacity maneuver in supine position. Evaluation of the respiratory MRI measures in a supine position is likely to be more sensitive in detecting early signs of the diaphragm weakness. We did not use an MR-compatible spirometer during scanning, and this could have potentially improved compliance of subjects. Our data indicate that particularly for patients, the overall variability in the repeated measurements came from differences between individuals, not within individuals. A negative correlation between patients' age and their chest wall motion and diaphragm contractility may demonstrate a trend for deterioration in these measures in older DMD patients. Longitudinal observations in a larger group of patients including younger boys and nonambulatory individuals may identify the most informative biomarkers for demonstrating the change in respiratory status in individual muscles overtime and to determine whether there is a difference with therapeutic intervention.

In conclusion, we show the feasibility of separate assessments of the diaphragm and chest wall muscles using MRI in younger boys with DMD and controls. Although respiratory morbidity is heralded by a decrease

in FVC according to current guidelines,³ the MRI data indicate that younger ambulatory DMD patients show signs of diminished lung areas at total lung capacity and residual volume when their FVC is determined to be within normal range. Our results demonstrate a reduction in chest wall motion and validate the common perception that the diaphragm is not affected at this early stage in DMD. The rate of progression in these parameters, their ability to predict the FVC decline, and whether early initiation of treatment has positive effects on the quality of life can be determined in future studies of DMD patients.

Acknowledgments

The study was supported by the Intramural Research Program of the National Institute of Neurological Disorders and Stroke, the National Institutes of Health Clinical Center, and the National Heart, Lung, and Blood Institute. The authors thank the study participants and their families; Donovan Stock, Elizabeth Hartnett, and Alice Schindler (NINDS) for help with coordinating study visits and scheduling MRI studies; Christine Mancini and Drs. Laura Olivieri and Sujata Shanbhag (NHLBI) for help with acquiring MRI data; and the principal investigators of the referring sites participating in the DMD114876 trial (NCT01462292; Drs. Barry Russman, Portland, OR; Benjamin Renfroe, Gulf Breeze, FL; Brenda Wong, Cincinnati, OH; Douglas Sproule, New York, NY; Edward Smith, Durham, NC; and Kathryn Wagner, Baltimore, MD) for sharing study participants. We thank Dr. Carsten Bönemann (NINDS) for helpful discussions about study concept and design. We also thank GlaxoSmithKline and Prosensa/BioMarin, study sponsors of the DMD114876 trial, for sharing the pulmonary function test results of patients at randomization visit.

Author Contribution

AM, GN, WPB, EK, KHF, AEA, and JY drafted and revised the manuscript for content; AM, KF, and AEA conceived the study; WPB and AEA carried out acquisition of imaging data; AM, WK, NH, CAB, HS, RN, and JY analyzed or interpreted the data; and GN and EK carried out statistical analysis.

Conflict of Interest

This study was supported by the Intramural Research Program of the National Institute of Neurological Disorders and Stroke, the National Heart, Lung, and Blood Institute, and the National Institutes of Health Clinical Center. Drs. Bishop and Newbould are employees of Imanova Limited

(London, UK). Dr. Arai reports nonfinancial support from Siemens (Erlangen, Germany), outside the submitted work; all other authors report no disclosures.

References

1. Finder JD, Birnkrant D, Carl J, et al. Respiratory care of the patient with Duchenne muscular dystrophy - ATS Consensus Statement. *Am J Respir Crit Care Med* 2004;170:456–465.
2. Eagle M, Baudouin SV, Chandler C, et al. Survival in Duchenne muscular dystrophy: improvements in life expectancy since 1967 and the impact of home nocturnal ventilation. *Neuromuscul Disord* 2002;12:926–929.
3. Bushby K, Finkel R, Birnkrant DJ, et al. Diagnosis and management of Duchenne muscular dystrophy, part 1: diagnosis, and pharmacological and psychosocial management. *Lancet Neurol* 2010;9:77–93.
4. Buyse GM, Voit T, Schara U, et al. Efficacy of idebenone on respiratory function in patients with Duchenne muscular dystrophy not using glucocorticoids (DELOS): a double-blind randomised placebo-controlled phase 3 trial. *Lancet* 2015;385:1748–1757.
5. Henricson EK, Abresch RT, Cnaan A, et al. The cooperative international neuromuscular research group Duchenne natural history study: glucocorticoid treatment preserves clinically meaningful functional milestones and reduces rate of disease progression as measured by manual muscle testing and other commonly used clinical trial outcome measures. *Muscle Nerve* 2013;48:55–67.
6. Crisp A, Yin H, Goyenvalle A, et al. Diaphragm rescue alone prevents heart dysfunction in dystrophic mice. *Hum Mol Genet* 2011;20:413–421.
7. Bushby K, Finkel R, Birnkrant DJ, et al. Diagnosis and management of Duchenne muscular dystrophy, part 2: implementation of multidisciplinary care. *Lancet Neurol* 2010;9:177–189.
8. Mayer OH, Finkel RS, Rummey C, et al. Characterization of pulmonary function in Duchenne muscular dystrophy. *Pediatr Pulmonol* 2015;50:487–494.
9. Fauroux B, Quijano-Roy S, Desguerre I, Khirani S. The value of respiratory muscle testing in children with neuromuscular disease. *Chest* 2015;147:552–559.
10. Allen SM, Hunt B, Green M. Fall in vital capacity with posture. *Br J Dis Chest* 1985;79:267–271.
11. Won YH, Choi WA, Kim DH, Kang SW. Postural vital capacity difference with aging in Duchenne muscular dystrophy. *Muscle Nerve* 2015;52:722–727.
12. Wens SC, Ciet P, Perez-Rovira A, et al. Lung MRI and impairment of diaphragmatic function in Pompe disease. *BMC Pulm Med* 2015;15:54.
13. Gaeta M, Musumeci O, Mondello S, et al. Clinical and pathophysiological clues of respiratory dysfunction in late-onset Pompe disease: New insights from a comparative

- study by MRI and respiratory function assessment. *Neuromuscul Disord* 2015;25:852–858.
14. Mankodi A, Bishop CA, Auh S, et al. Quantifying disease activity in fatty-infiltrated skeletal muscle by IDEAL-CPMG in Duchenne muscular dystrophy. *Neuromuscul Disord* 2016;26:650–658.
 15. Gaur L, Hanna A, Bandettini WP, et al. Upper arm and cardiac magnetic resonance imaging in Duchenne muscular dystrophy. *Ann Clin Transl Neurol* 2016;3:948–955.
 16. Breuer FA, Kellman P, Griswold MA, Jakob PM. Dynamic autocalibrated parallel imaging using temporal GRAPPA (TGRAPPA). *Magn Reson Med* 2005;53:981–985.
 17. LeCun Y, Bengio Y, Hinton G. Deep learning. *Nature* 2015;521:436–444.
 18. Roth HR, Le Lu, Farag A, Sohn A, Summers RM. Spatial aggregation of holistically-nested networks for automated pancreas segmentation. Presented at the 19th Medical Image Computing and Computer-Assisted Intervention (MICCAI) 17 - 21 October, 2016; Athens, Greece. Available at: <http://arxiv.org/abs/1606.07830>
 19. Simonyan K, Zisserman A. Very deep convolutional networks for large-scale image recognition. Presented at the 3rd International Conference on Learning Representations. 1556, 7 - 9 May, 2015; San Diego, CA. Available at: <http://arxiv.org/abs/1409>
 20. Deng J, Dong W, Socher R, Li LJ, Li K, Li FF. ImageNet: a large-scale hierarchical image database. *IEEE Comput Vis Pattern Recogn (CVPR)*. 2009;1–4: 248–255
 21. Shin HC, Roth HR, Gao MC, et al. Deep convolutional neural networks for computer-aided detection: CNN architectures, dataset characteristics and transfer learning. *IEEE Trans Med Imaging* 2016;35:1285–1298.
 22. Kondo T, Kobayashi I, Taguchi Y, Ohta Y, Yanagimachi N. A dynamic analysis of chest wall motions with MRI in healthy young subjects. *Respirology* 2000;5:19–25.
 23. Bland JM, Altman DG. Statistical methods for assessing agreement between two methods of clinical measurement. *Lancet* 1986;1:307–310.
 24. Stehling F, Dohna-Schwake C, Mellies U, Grosse-Onnebrink J. Decline in lung volume with Duchenne muscular dystrophy is associated with ventilation inhomogeneity. *Respir Care* 2015;60:1257–1263.
 25. Hahn A, Bach JR, Delaubier A, Renardel-Irani A, Guillou C, Rideau Y. Clinical implications of maximal respiratory pressure determinations for individuals with Duchenne muscular dystrophy. *Arch Phys Med Rehabil* 1997;78:1–6.
 26. Owens MW, Kinasewitz GT, Anderson WM. Clinical significance of an isolated reduction in residual volume. *Am Rev Respir Dis* 1987;136:1377–1380.
 27. Cook CD, Hamann JF. Relation of lung volumes to height in healthy persons between the ages of 5 and 38 years. *J Pediatr* 1961;59:710–714.
 28. Whitehead NP, Bible KL, Kim MJ, Odom GL, Adams ME, Froehner SC. Validation of ultrasonography for non-invasive assessment of diaphragm function in muscular dystrophy. *J Physiol* 2016;594:7215–7227.
 29. Ayoub J, Milane J, Targhetta R, et al. Diaphragm kinetics during pneumatic belt respiratory assistance: a sonographic study in Duchenne muscular dystrophy. *Neuromuscul Disord* 2002;12:569–575.
 30. Mogalle K, Perez-Rovira A, Ciet P, et al. Quantification of diaphragm mechanics in Pompe disease using dynamic 3D MRI. *PLoS ONE* 2016;11:e0158912.
 31. Sivak ED, Salanga VD, Wilbourn AJ, Mitsumoto H, Golish J. Adult-onset acid maltase deficiency presenting as diaphragmatic paralysis. *Ann Neurol* 1981;9:613–615.
 32. Estenne M, Gevenois PA, Kinnear W, Soudon P, Heilporn A, De Troyer A. Lung volume restriction in patients with chronic respiratory muscle weakness: the role of microatelectasis. *Thorax* 1993;48:698–701.

Supporting Information

Additional Supporting Information may be found online in the supporting information tab for this article:

Video S1. Dynamic changes of the lung area and the diaphragm during maximal breathing in the coronal plane during 10 sec of cine MRI recording in a patient with Duchenne muscular dystrophy (A) and an age-matched healthy volunteer boy (B).

Video S2. Dynamic changes of the lung area and the diaphragm during maximal breathing in the right sagittal plane during 10 sec of cine MRI recording in a patient with Duchenne muscular dystrophy (A) and an age-matched healthy volunteer boy (B).